

A multi-messenger hierarchical triple merger gravitational-wave event pair GW190514-GW190521 inside AGN J124942.3 + 344929

Guo-Peng Li¹ and Xi-Long Fan^{1,*}

¹*Department of Astronomy, School of Physics and Technology, Wuhan University, Wuhan 430072, China*
(Dated: March 24, 2025)

There is a candidate electromagnetic counterpart to the binary black hole merger GW190521, identified as ZTF19abanrhr within AGN J124942.3 + 344929. Additionally, GW190514 is proposed as a plausible precursor merger to GW190521 within a hierarchical merger scenario. In this study, we investigate the potential association between GW190514 and GW190521 as a hierarchical triple merger associated with ZTF19abanrhr, taking into account of sky position, distance, and mass of the sources using a Bayesian criterion. Our analysis reveals that the association is favored over a random coincidence, with a log Bayes factor of 16.8, corresponding to an odds ratio of $\sim 199 : 1$, assuming an astrophysical prior odds of 10^{-5} . Notably, when accounting for the primary masses of the two gravitational wave events as potential products of mergers in the AGN formation channel, the Bayes factor increases significantly, further enhancing the preference for this association by a factor of $\sim 10^2$, corresponding to a log Bayes factor of 21.5 and an odds ratio of $\sim 2 \times 10^4 : 1$. Our results suggest strong evidence for the first hierarchical triple merger associated with an electromagnetic counterpart in the AGN formation channel. This work is crucial for understanding the formation mechanisms of massive black holes, the role of AGNs in hierarchical mergers, and the implications of multi-messenger astronomy.

I. INTRODUCTION

GW190521 [1] is one of the most massive binary black hole merger observed during the first three LIGO-Virgo observing runs, with component masses of approximately $85 M_{\odot}$ and $66 M_{\odot}$, producing a remnant black hole of around $142 M_{\odot}$, which can be classified as an intermediate mass black hole. GW190514 [2] is another binary black hole merger, with component masses of approximately $39 M_{\odot}$ and $28 M_{\odot}$, resulting in remnant black hole of around $67 M_{\odot}$, which overlaps with the second mass range of GW190521. Moreover, there is significant spatial overlap between the sky localizations and distances of GW190514 and GW190521 (see Fig. 1), suggesting a plausible scenario where these two events are part of a hierarchical triple merger. In this scenario, GW190514 would represent the first merger, producing a remnant black hole that later paired with another black hole to form the hierarchical system responsible for GW190521 [3].

In addition, an optical electromagnetic counterpart candidate, ZTF19abanrhr, was reported by Graham *et al.* [4], detected by the Zwicky Transient Facility approximately 34 days after the gravitational wave event GW190521. Evidence in favor of an association between the gravitational wave event and the electromagnetic counterpart was also reported in [5, 6] (although [7, 8]) This counterpart, confirmed as a flare within the active galactic nuclei (AGN) AGN J124942.3 + 344929, was at the 78% spatial contour for GW190521's sky localization. Interestingly, GW190514's

90% sky localization also coincides with the position of ZTF19abanrhr (see Fig. 1). This raises an intriguing question: Could both GW190514 and GW190521 be a hierarchical triple merger originating from AGN J124942.3 + 344929, with ZTF19abanrhr serving as their electromagnetic counterpart?

Theoretical models suggest that AGN disks are promising environments for massive and hierarchical binary black hole mergers [9–11], consistent with the observed events GW190514 and GW190521. In such environments, electromagnetic emissions are expected, likely produced by shocks from accreting merger remnants interacting with the baryon-rich, high-density surroundings [12–15]. Additionally, AGN disks could facilitate an excess of eccentric mergers, which may provide a possible explanation for the non-zero eccentricity and significant spin-orbit tilt of GW190521 if it originated in such an environment [16]. Moreover, the final mass of GW190514 is consistent with the best-matching eccentric template for GW190521's mass distribution [3].

Motivated by this, we propose a compelling scenario: GW190514, detected by the Advanced LIGO [17], represents a first generation black hole merger occurring within AGN J124942.3 + 344929, which left behind a remnant black hole that rapidly merged with another black hole, facilitated by interactions with the gas, leading to the formation of GW190521, detected by the Advanced LIGO and the Advanced Virgo [18]. Concurrently, the accreting remnant black hole from either GW190521 or GW190514 produced an optical flare ZTF19abanrhr, which was observed by the Zwicky Transient Facility [19] approximately 40 days after the merger [4, 20].

The rest of this paper is organized as follows. In Section II, we provide a description of the methodology used in this study. In Section III, we present the results of our

* Corresponding author: Xi-Long Fan
xilong.fan@whu.edu.cn

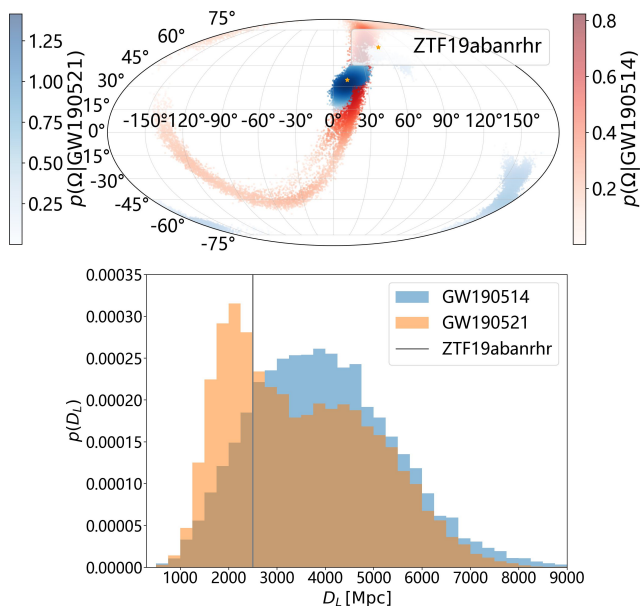


FIG. 1. Probability distribution of the sky position and distance. Top: Mollweide projection of the sky positions of GW190514 (red), GW190521 (blue), and ZTF19abnrhr (orange) within AGN J124942.3 + 344929. ZTF19abnrhr lies within the 78% spatial contour for GW190521’s sky localization, while GW190514’s 90% sky localization is consistent with the position of ZTF19abnrhr. Bottom: Marginalized luminosity distance distributions integrated over the sky for GW190514 (blue) and GW190521 (yellow). The luminosity distance (gray) of ZTF19abnrhr is derived from the redshift $z = 0.438$ of AGN J124942.3 + 344929, assuming a Planck18 cosmology [21].

analysis. We conclude with our discussion in Section IV.

II. METHODS

We explore the potential association between GW190514 and GW190521 as hierarchical triple merger in AGN J124942.3 + 344929, associated with ZTF19abnrhr, using data (d_1 and d_2 for the gravitational signals¹, and s for the electromagnetic signal²) from the GWTC-2.1 release [2] and ZTF [19]. This is a hypothesis-testing question. Our analysis employs a Bayesian criterion to assess whether signals observed from these separate data sets share a common origin. The association (\mathcal{H}_1) at least requires that i) the localizations of GW190514, GW190521, and ZTF19abnrhr must be consistent (see Fig. 1); and ii) the final mass of GW190514 should align with the second mass in GW190521. In contrary, the coincidence (\mathcal{H}_0) corresponds to the scenario where the three

detections are associated by chance. As a result, the odds \mathcal{O}_0^1 between the hypotheses \mathcal{H}_1 and \mathcal{H}_0 is given by: $\mathcal{O}_0^1(d_1, d_2, s) = \mathcal{P}_0^1 \mathcal{B}_0^1(d_1, d_2, s)$, where \mathcal{P}_0^1 is the *prior odds*; and $\mathcal{B}_0^1(d_1, d_2, s) = p(d_1, d_2, s | \mathcal{H}_1) / p(d_1, d_2, s | \mathcal{H}_0)$ is the *Bayes factor* defined by the ratio of the evidences of the hypotheses.

The derivations and computational framework presented as follows build upon the foundational methodology established in Morton *et al.* [5], who demonstrated the astrophysical association between GW190521 and flare ZTF19abnrhr as its electromagnetic counterpart. Here we investigate the association between GW190514 and GW190521 as a hierarchical triple merger associated with ZTF19abnrhr.

A. Environmental effects

Stellar-mass binary black holes residing in AGN disks near the central supermassive black hole are influenced by various environmental effects. These effects can introduce biases in the parameter estimates of gravitational wave events, particularly altering the observed mass and distance of sources. Following the analysis in the previous literature [5], both effects impact the properties of the sources.

The first effect, related to the gravitational potential of the supermassive black hole, leads to gravitational redshift.

$$z_{\text{grav}} = \left(1 - \frac{R_s}{r}\right)^{1/2} - 1, \quad (1)$$

where R_s represents the Schwarzschild radius of the supermassive black hole, and r is the distance between the binary black hole and the supermassive black hole. The gravitational redshift is calculated assuming a non-spinning supermassive black hole, although supermassive black holes in AGN disks are typically expected to spin [22]. This assumption holds because the effect of spin becomes negligible at the distances relevant for binary black holes with respect to the supermassive black hole [23–25].

The second effect, which is related to the motion of the binary black hole as it orbits the supermassive black hole, results in a relativistic redshift,

$$z_{\text{rel}} = \gamma [1 + v \cos(\phi)] - 1, \quad (2)$$

where $\gamma = (1 - v^2)^{-1/2}$ is the Lorentz factor, v is the magnitude of the velocity, and ϕ is the viewing angle between the velocity and the line of sight in the observer frame. Assuming that the binary black hole is on a circular orbit around a non-spinning supermassive black hole [26], its velocity is

$$v = \frac{1}{\sqrt{2(r/R_s - 1)}}. \quad (3)$$

¹ <https://zenodo.org/record/5117702>

² <https://lasair-ztf.lsst.ac.uk/objects/ZTF19abnrhr/>

Note that [5] the degeneracy between the mass of the source and the relativistic redshift remains unresolved because detection is mainly done with the dominant quadrupolar mode [27]. However, the ambiguity between the relativistic redshift and other redshifts can be eliminated by detecting higher spherical modes, thus allowing, in principle, for the measurement of the source's velocity [28–30].

In this case, the detected mass of a redshifted source differs from intrinsic mass in the source frame by a factor equal to the combined effects of all relevant redshifts, including gravitational and relativistic redshifts [31],

$$m^{z,\text{eff}} = (1 + z_{\text{grav}})(1 + z_{\text{rel}}) m^z, \quad (4)$$

where $m^{z,\text{eff}}$ represents the observed mass of the source in the detector frame, $m^z = (1 + z_c) m$ is the observed mass with the cosmological redshift z_c , in which m is the intrinsic mass in the source frame.

The effective distance of the source is also influenced by various redshift effects, with the relativistic redshift component, induced by the aberration of gravitational waves, being squared in its impact on the observed distance [32].

$$D_L^{\text{eff}} = (1 + z_{\text{grav}})(1 + z_{\text{rel}})^2 D_L, \quad (5)$$

where $D_L = (1 + z_c) D_{\text{com}}$ is the luminosity distance of the source with D_{com} the comoving distance between source and observer.

Consequently, the environmental effects of the supermassive black hole, such as gravitational and relativistic redshifts, can be accounted for by simply replacing the observed mass m^z with the effective mass $m^{z,\text{eff}}$, and the luminosity distance D_L with the effective luminosity distance D_L^{eff} [5].

B. Bayesian criterion

In order to assess whether it is more likely that the two gravitational wave events, GW190514 and GW190521 (as

$$p(d_1, d_2, s | \mathcal{H}_i) = \int dD_L d\Omega dm^z p(d_1, d_2, s | D_L, \Omega, m^z, \mathcal{H}_i) p(D_L, \Omega, m^z | \mathcal{H}_i). \quad (9)$$

The first term of equation (9),

$$p(d_1, d_2, s | D_L, \Omega, m^z, \mathcal{H}_i) \propto \frac{p(D_L, \Omega, m^z | d_1, \mathcal{H}_i)}{p(D_L, \Omega, m^z | \mathcal{H}_i)} \frac{p(D_L, \Omega, m^z | d_2, \mathcal{H}_i)}{p(D_L, \Omega, m^z | \mathcal{H}_i)} \frac{p(D_L, \Omega | s, \mathcal{H}_i)}{p(D_L, \Omega | \mathcal{H}_i)}, \quad (10)$$

where $p(D_L, \Omega, m^z | d_i, \mathcal{H}_i)$ is the posterior probability

density for the gravitational wave data set d_i (as well as the electromagnetic transient ZTF19abnrhr, originate from a common source, or whether the three detections are associated by chance, we employ a Bayesian statistical analysis. Given three detections in the GW190514 data set d_1 , the GW190521 data set d_2 , and the ZTF19abnrhr data set s , the odds \mathcal{O}_0^1 between the association model \mathcal{H}_1 and the coincidence model \mathcal{H}_0 is given by:

$$\mathcal{O}_0^1(d_1, d_2, s) = \frac{p(\mathcal{H}_1 | d_1, d_2, s)}{p(\mathcal{H}_0 | d_1, d_2, s)} = \frac{p(d_1, d_2, s | \mathcal{H}_1) p(\mathcal{H}_1)}{p(d_1, d_2, s | \mathcal{H}_0) p(\mathcal{H}_0)}. \quad (6)$$

Here

$$\mathcal{B}_0^1(d_1, d_2, s) = \frac{p(d_1, d_2, s | \mathcal{H}_1)}{p(d_1, d_2, s | \mathcal{H}_0)}, \quad (7)$$

is the *Bayes factor* and $\mathcal{P}_0^1 = p(\mathcal{H}_1)/p(\mathcal{H}_0)$ is the *prior odds*. The prior odds for the two models can be simplified as the product of two parts: 1) the odds for the electromagnetic transient associated with one of the two gravitational wave events is $\sim 1/13$ [8], obtained from the fact that there are approximately ≈ 13 events similar to ZTF19abnrhr in the Zwicky Transient Facility alert stream over the given observing epoch [4]; 2) the odds for any two gravitational wave events detected by LIGO and Virgo being a hierarchical triple merger is $\sim 1/1000$ [33] corresponding to the proportion of hierarchical merger events within the total population of detectable mergers in the optimistic scenario [34]. As a result, we adopt a conservative estimate for the astrophysical prior odds $\mathcal{P}_0^1 \sim 10^{-5}$.

The Bayes factor is the ratio of the evidences for the two hypothetical models. The evidence for a model can be computed via the marginalization over all parameters $\vec{\theta}$ required by the model \mathcal{H}_i ,

$$p(d_1, d_2, s | \mathcal{H}_i) = \int d\vec{\theta} p(d_1, d_2, s | \vec{\theta}, \mathcal{H}_i) p(\vec{\theta} | \mathcal{H}_i). \quad (8)$$

The parameters of interest for this work are the sky localization Ω and luminosity distance D_L of the three sources, and the overlap mass m^z in the detector frame, which refers to the final mass of GW190514 and to the second mass of GW190521. One has

$p(d_1, d_2, s | D_L, \Omega, m^z, \mathcal{H}_i)$ can be written as

density for the gravitational wave data set d_i

and $p(D_L, \Omega, m^z | \mathcal{H}_i) = p(D_L, \Omega | \mathcal{H}_i) p(m^z | \mathcal{H}_i) = p(D_L | \mathcal{H}_i) p(\Omega | \mathcal{H}_i) p(m^z | \mathcal{H}_i)$ is the prior probability distribution used during the parameter estimation run by the LIGO-Virgo-KAGRA (LVK) Collaboration. The parameter estimation prior is uniform in the sky localization and mass, and in the square of the luminosity distance. The possible travel between the mergers is neglected [3]. The probability density $p(D_L, \Omega | s, \mathcal{H}_i) = p(D_L | s, \mathcal{H}_i) p(\Omega | s, \mathcal{H}_i)$ is obtained from the localization of its host AGN J124942.3 + 344929. The conversion in $p(D_L | s, \mathcal{H}_i)$ between luminosity distance and redshift takes into account environmental effects, which are discussed in detail in the corresponding models below.

The second term in equation (9), $p(D_L, \Omega, m^z | \mathcal{H}_i)$, is the prior conditioned under the hypothetical model \mathcal{H}_i . In general, these parameters are a *priori* independent,

we can factorize it as

$$p(D_L, \Omega, m^z | \mathcal{H}_i) = p(D_L | \mathcal{H}_i) p(\Omega | \mathcal{H}_i) p(m^z | \mathcal{H}_i), \quad (11)$$

where the prior $p(m^z | \mathcal{H}_i)$ differs in the different models. In the association model \mathcal{H}_1 , $p(m^z | \mathcal{H}_1) = p_{m_f}^{1g}(m^z | \mathcal{H}_1)$ represents the final detector-frame mass distributions of first generation binary black hole mergers that are not a result of a previous merger in the AGN formation channel. In the coincidence model \mathcal{H}_0 , $p(m^z | \mathcal{H}_0) = p_{m_f}^{1g}(m^z | \mathcal{H}_0)$ and $p(m^z | \mathcal{H}_0) = p_{m_2}^{\text{hier}}(m^z | \mathcal{H}_0)$ refer to the final mass distributions of first-generation binary black hole mergers and the second mass distributions of hierarchical binary black hole mergers, respectively, in the detector frame, for formation channels other than AGN disks.

Substituting equations (10)&(11) into equation (9):

$$\begin{aligned} p(d_1, d_2, s | \mathcal{H}_1) &= \int dD_L d\Omega dm^z \frac{p(D_L, \Omega, m^z | d_1, \mathcal{H}_1)}{p(D_L | \mathcal{H}_1) p(\Omega | \mathcal{H}_1) p(m^z | \mathcal{H}_1)} \frac{p(D_L, \Omega, m^z | d_2, \mathcal{H}_1)}{p(D_L | \mathcal{H}_1) p(\Omega | \mathcal{H}_1) p(m^z | \mathcal{H}_1)} \\ &\quad \times \frac{p(D_L, \Omega | s, \mathcal{H}_1)}{p(D_L | \mathcal{H}_1) p(\Omega | \mathcal{H}_1)} p(D_L | \mathcal{H}_1) p(\Omega | \mathcal{H}_1) p_{m_f}^{1g}(m^z | \mathcal{H}_1) \\ &= \int dD_L d\Omega dm^z \frac{p(D_L, \Omega, m^z | d_1, \mathcal{H}_1) p(D_L, \Omega, m^z | d_2, \mathcal{H}_1) p(D_L | s, \mathcal{H}_1) p(\Omega | s, \mathcal{H}_1)}{p^2(D_L | \mathcal{H}_1) p^2(\Omega | \mathcal{H}_1) p^2(m^z | \mathcal{H}_1)} p_{m_f}^{1g}(m^z | \mathcal{H}_1), \end{aligned} \quad (12)$$

and

$$\begin{aligned} p(d_1, d_2, s | \mathcal{H}_0) &= \int dD_L d\Omega dm^z \frac{p(D_L, \Omega, m^z | d_1, \mathcal{H}_0)}{p(D_L | \mathcal{H}_0) p(\Omega | \mathcal{H}_0) p(m^z | \mathcal{H}_0)} p(D_L | \mathcal{H}_0) p(\Omega | \mathcal{H}_0) p_{m_f}^{1g}(m^z | \mathcal{H}_0) \\ &\quad \times \int dD_L d\Omega dm^z \frac{p(D_L, \Omega, m^z | d_2, \mathcal{H}_0)}{p(D_L | \mathcal{H}_0) p(\Omega | \mathcal{H}_0) p(m^z | \mathcal{H}_0)} p(D_L | \mathcal{H}_0) p(\Omega | \mathcal{H}_0) p_{m_2}^{\text{hier}}(m^z | \mathcal{H}_0) \\ &\quad \times \int dD_L d\Omega \frac{p(D_L, \Omega | s, \mathcal{H}_0)}{p(D_L | \mathcal{H}_0) p(\Omega | \mathcal{H}_0)} p(D_L | \mathcal{H}_0) p(\Omega | \mathcal{H}_0) \\ &= \int dm^z \frac{p(m^z | d_1, \mathcal{H}_0)}{p(m^z)} p_{m_f}^{1g}(m^z | \mathcal{H}_0) \times \int dm^z \frac{p(m^z | d_2, \mathcal{H}_0)}{p(m^z)} p_{m_2}^{\text{hier}}(m^z | \mathcal{H}_0). \end{aligned} \quad (13)$$

The second equal sign arises from the fact that the integrals over the spatial localization in equation (13) equal unity and are therefore omitted.

For comparison, we also investigate scenarios where only two detections share a common source, instead of all three, by removing irrelevant observation data from equations (12)&(13). Specifically, for three detections (a , b , and c), we define the model $\{a, b, c\}$ as corresponding to \mathcal{H}_0 , meaning the three detections are unrelated, while the model $\{a-b-c\}$ corresponds to \mathcal{H}_1 , meaning they share a common origin. The model $\{a-b, c\}$ includes three different combinations, denoted as \mathcal{H}_2 , \mathcal{H}_3 , and \mathcal{H}_4 (see Table I). In the following sections, we introduce the pre-

descriptions for the distributions $p(D_L | s)$ and $p(m^z | \mathcal{H}_i)$ under the two hypothetical models.

C. Association model

In the association model \mathcal{H}_1 , the gravitational wave events GW190514 and GW190521, as a hierarchical triple merger, and the flare ZTF19abanrh share a common origin. The localization is fixed to the host AGN J124942.3 + 344929, and as a result, the observed mass and distance of the source are altered due to environmental effects. In this case, the gravitational wave posterior probability

densities used in our work are the detector-frame effective primary mass $m^{z,\text{eff}}$ and effective luminosity distance D_L^{eff} . These two parameters are independently measured in gravitational wave detection; however, under the com-

mon origin hypothesis, they depend on the additional redshifts introduced by environmental effects.

The luminosity distance of the electromagnetic source is expressed as $p(D_L|s, \mathcal{H}_1) \rightarrow p(D_L^{\text{eff}}|s, \mathcal{H}_1)$:

$$p(D_L^{\text{eff}}|s, \mathcal{H}_1) = \int dD_L dr d\phi \delta [D_L^{\text{eff}} - (1 + z_{\text{grav}}(r)) (1 + z_{\text{rel}}(r, \phi))^2 D_L] p(D_L|s, \mathcal{H}_1) p(r) p(\phi), \quad (14)$$

where

$$p(D_L|s, \mathcal{H}_1) = \int dz p(D_L|z, \Omega_{\text{cosm}}) p(z|s, \mathcal{H}_1) \quad (15)$$

with Ω_{cosm} a set of cosmological parameters assuming a Planck18 cosmology for Ω_{cosm} [21], and

$$p(z|s, \mathcal{H}_1) = \delta(z - z_{\text{AGN}}) \quad (16)$$

the redshift $z_{\text{AGN}} = 0.438$ of AGN J124942.3 + 344929³. The expressions for $z_{\text{grav}}(r)$ and $z_{\text{rel}}(r, \phi)$ in equation (14) are the ones in equations (1) and (2), respectively. Here we adopt the prior $p(\phi)$ to be uniform in $\cos(\phi)$. The

radial distance prior, $p(r)$, between the binary black hole and the supermassive black hole is predicted based on migration traps in AGN disks [35]. We assume that this radial distance is uniformly distributed between 24.5 and 331 Schwarzschild radii [35]. It is important to note that the precise location of migration traps can vary depending on the disk model, and in some cases, there may not be a migration trap at all [36–38]. However, our results are robust and are not significantly affected by these uncertainties [5].

In the same way, the prior conditioned under the hypothetical model \mathcal{H}_1 reads $p(m^z|\mathcal{H}_1) \rightarrow p(m^{z,\text{eff}}|\mathcal{H}_1)$:

$$p(m^{z,\text{eff}}|\mathcal{H}_1) = \int dm dr d\phi \delta [m^{z,\text{eff}} - (1 + z_{\text{grav}}(r)) (1 + z_{\text{rel}}(r, \phi))(1 + z_c) m] p(m|\mathcal{H}_1) p(r) p(\phi), \quad (17)$$

where the cosmological redshift $z_c \equiv z_{\text{AGN}}$ and $p(m^z|\mathcal{H}_1) = (1 + z_c) p(m|\mathcal{H}_1)$. The astrophysical prior $p(m|\mathcal{H}_1)$ represents the mass distribution of BBHs formed in AGN disks, which is presented in the Appendix II E.

D. Coincidence model

In the coincidence model \mathcal{H}_0 , the three transients GW190514, GW190521, and ZTF19abnrhr are unrelated and happen to appear within the same localization by chance. In this scenario, there are no environmental effects from AGNs, and therefore, the only redshift present is the cosmological one. As a result, the prior conditioned under the hypothetical model \mathcal{H}_0 is given by,

$$p(m^z|\mathcal{H}_0) = (1 + z_c) p(m|\mathcal{H}_0), \quad (18)$$

where $p(m|\mathcal{H}_0)$ refers to the mass distribution of BBHs formed from channels other than AGN disks, discussed

below.

E. Astrophysical distributions

To obtain the astrophysical distributions, we utilize a phenomenological population model introduced in Li *et al.* [11], which allows for the rapid simulation of binary black hole mergers parametrized, including hierarchical mergers, within dynamical formation channels. For the first-generation binary black hole merger distributions, we adopt the results from the analysis of GWTC-3 by the LVK Collaboration [39]. In particular, the primary masses of binary black hole mergers that do not result from a previous merger follow a distribution described by a POWERLAW+PEAK model. The parameters of the POWERLAW+PEAK model used for the coincidence model \mathcal{H}_0 are consistent with the results of GWTC-3. For the association model \mathcal{H}_1 , the mass power-law index aligns with predictions for a top-heavy population of merging black holes in AGN disks [40]. The dimensionless spin-magnitude distribution of first-generation black holes is uniformly assigned within a beta distribution. In the model \mathcal{H}_0 , its parameters are obtained from the GWTC-3, while the parameters determining the distribution's mean and variance are set to 1.5 and 3.0 in the

³ <https://skyserver.sdss.org/dr12/en/tools/explore/Summary.aspx?id=1237665128546631763>

model \mathcal{H}_1 , reflecting the angular momentum exchange between binaries and the disk [41]. In both models, the spin tilt angles are randomly selected from an isotropic distribution across a sphere.

In order to pair binary black holes, the mass ratios of the binaries are drawn from a POWERLAW distribution. Similarly, in the model \mathcal{H}_0 , we take the mass-ratio power-law parameter from the GWTC-3, setting it to be ~ 0 in the model \mathcal{H}_1 , which represents the expectations of a runaway merger scenario in AGN disks [10]. We assume an NG+ \leq NG branch for hierarchical mergers (see details in Li *et al.* [11]). We use numerical relativity fits to calculate each merger remnant's final mass, final spin, and

kick velocity [42–44]. To ensure that our results are not impacted by the potential parameter values used above, we repeated the analysis with variations of these parameters and found that our results do not strongly depend on them.

F. Models including primary masses

Following the considerations from previous literature, we take the primary masses of gravitational wave events into account in our hypothetical models [5]. The equations (12) and (13) become

$$\begin{aligned}
 p(d_1, d_2, s | \mathcal{H}_1) &= \int dD_L d\Omega dm^z dm'^z dm''^z \\
 &\times \frac{p(D_L, \Omega, m^z, m'^z | d_1, \mathcal{H}_1) p(D_L, \Omega, m^z, m''^z | d_2, \mathcal{H}_1) p(D_L | s) p(\Omega | s, \mathcal{H}_1)}{p^2(D_L | \mathcal{H}_1) p^2(\Omega | \mathcal{H}_1) p^2(m^z | \mathcal{H}_1) p(m'^z | \mathcal{H}_1) p(m''^z | \mathcal{H}_1)} \\
 &\times p_{m_f}^{\text{lg}}(m^z | \mathcal{H}_1) p_{m_1}^{\text{lg}}(m'^z | \mathcal{H}_1) p_{m_1}^{\text{hier}}(m''^z | \mathcal{H}_1),
 \end{aligned} \tag{19}$$

and

$$\begin{aligned}
 p(d_1, d_2, s | \mathcal{H}_0) &= \int dm^z dm'^z \frac{p(m^z, m'^z | d_1, \mathcal{H}_0)}{p(m^z | \mathcal{H}_0) p(m'^z | \mathcal{H}_0)} p_{m_f}^{\text{lg}}(m^z | \mathcal{H}_0) p_{m_1}^{\text{lg}}(m'^z | \mathcal{H}_0) \\
 &\times \int dm^z dm''^z \frac{p(m^z, m''^z | d_2, \mathcal{H}_0)}{p(m^z | \mathcal{H}_0) p(m''^z | \mathcal{H}_0)} p_{m_2}^{\text{hier}}(m^z | \mathcal{H}_0) p_{m_1}^{\text{hier}}(m''^z | \mathcal{H}_0),
 \end{aligned} \tag{20}$$

where m'^z and m''^z are the primary masses of GW190514 and GW190521 in the detector frame, respectively; $p(m'^z | \mathcal{H}_1)$ and $p(m''^z | \mathcal{H}_1)$ are the priors used during the parameter estimation run; and $p_{m_1}^{\text{lg}}(m'^z | \mathcal{H}_1)$ and $p_{m_1}^{\text{hier}}(m''^z | \mathcal{H}_1)$ ($p_{m_1}^{\text{lg}}(m'^z | \mathcal{H}_0)$ and $p_{m_1}^{\text{hier}}(m''^z | \mathcal{H}_0)$) are the priors conditioned of primary detector-frame masses of first generation and hierarchical mergers in the AGN formation channel (in formation channels other than AGN disks), respectively.

III. RESULTS

Figure 2 shows the posterior probability densities for the final mass of GW190514 and the second mass of GW190521, alongside the association model (labeled as ‘Association’, red). The distribution for the association model is more tightly constrained with respect to the coincidence model (as the GWTC-2.1 distribution [2]). Making use of the standard Bayesian Monte Carlo sampling algorithms, we perform model selection by calculating the evidence for each hypothesis. Accounting for the environmental effects, the log Bayes factor is $\log \mathcal{B} = 16.8$,

corresponding to an odds ratio of $\mathcal{O} \sim 199 : 1$, assuming an astrophysical prior odds of $\mathcal{P} \sim 10^{-5}$, which strongly supports the common origin hypothesis. Through specific analysis, we find that the Bayes factor is driven by two major contributions: i) the consistent localizations, and ii) the different mass priors for the two models. In particular, the log Bayes factors is $\log \mathcal{B} = 8.7$ when considering localizations alone. In addition, to ensure that our results are not biased by differing astrophysical priors or by the absence of the mass gap (caused by (pulsational) pair-instability supernovae [45, 46]) which are less likely in AGN disks due to increased probabilities for hierarchical mergers and accretion [5], we repeated the analysis using a mass model without the mass gap as the prior for the coincidence model, yielding a similar result.

Furthermore, we find that the primary masses of these two gravitational wave events are also crucial for enhancing the probability of the association compared to the coincidence [5]. This is because binary black hole mergers in AGN disks are generally expected to have more massive components compared to other channels, such as isolated binary evolution or star clusters, due to ac-

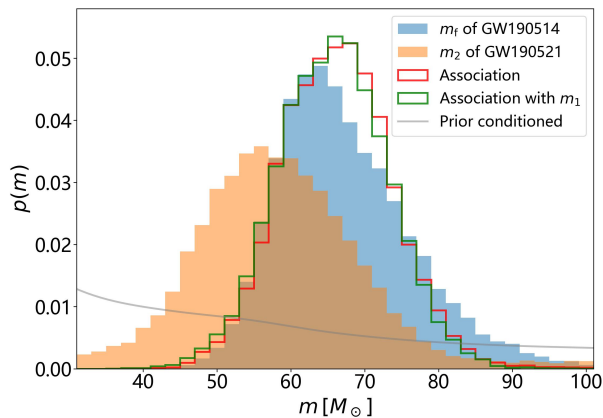


FIG. 2. Probability distribution of the associated mass. The empty histograms, each normalized, illustrate the associated mass distribution of GW190514-GW190521 for the association model, both without (red) and with (green) the inclusion of the primary mass m_1 . In contrast, the filled histograms represent the final mass distribution of GW190514 (blue) and the second mass distribution of GW190521 (yellow), as obtained from the GWTC-2.1. The gray line indicates the mass prior conditioned for the association model, which corresponds to the final mass distribution of the first generation binary black hole mergers in the AGN formation channel.

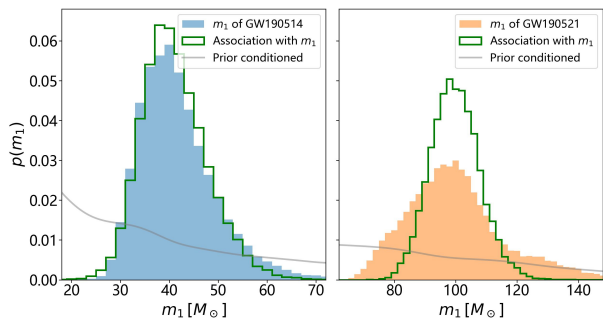


FIG. 3. Probability distribution of the primary mass. The empty histograms, each normalized, represent the primary mass distribution for the association model (green). For comparison, the filled histograms depict the primary mass distribution from the GWTC-2.1. The gray line indicates the mass prior conditioned for the association model. On the left, the distributions for GW190514 are displayed, with the prior conditioned corresponding to the primary mass distribution of first generation binary black hole mergers in the AGN formation channel. On the right, the distributions for GW190521 are shown, with the prior conditioned reflecting the primary mass distribution of hierarchical binary black hole mergers in the AGN formation channel.

cretion and frequent hierarchical mergers [9–11]. Therefore, we also consider the primary masses (m_1) of the gravitational wave events to assess the multi-messenger coincidence significance for the three transients (see Section II F). Figure 3 presents the posterior probability densities of the primary masses of the two gravitational wave events, comparing the distributions from the GWTC-

2.1 [2] with those from the association model (labeled as ‘Association with m_1 ’, green). As shown in this figure, the association model with m_1 provides better constraints, slightly favoring a more massive black hole for GW190521 and a less massive one for GW190514, compared to the GWTC-2.1 distributions [2]. Notably, GW190521’s primary black hole mass falls within the mass gap with nearly 100% probability, strongly suggesting that it is a hierarchical merger [47], potentially a second (or higher) generation merger resulting from GW190514 in an AGN environment. Incorporating the primary mass information significantly strengthens the association hypothesis, increasing the Bayes factor by approximately two orders of magnitude, corresponding to a log Bayes factor of $\log \mathcal{B} = 21.5$ and an odds ratio of $\mathcal{O} \sim 2 \times 10^4 : 1$. This result aligns with the expectation that more massive binary black hole mergers are more likely to occur in the AGN formation channel [9–11]. Additionally, we find that the inclusion of primary mass data allows slightly for better constraints on the associated mass between GW190514 and GW190521 (labeled as ‘Association with m_1 ’, green, in Fig. 2).

Finally, we note that in addition to the three detection associations, there may also be scenarios where only two detections share a common source. For comparison, we also investigate the scenarios, which has three different combinations, corresponding to the hypotheses \mathcal{H}_2 , \mathcal{H}_3 , and \mathcal{H}_4 in Table I. Table I presents the Bayes factors and odds for various association combinations of GW190514, GW190521, and ZTF19abannhr, indicating that a common origin shared by the three transients is strongly favored based on the observed data sets, in contrast to the associations involving only two of them. In particular, the odds of \mathcal{H}_1 is ~ 14 (3902) times greater than the odds of \mathcal{H}_2 , \mathcal{H}_3 , and \mathcal{H}_4 (considering the primary masses). The analysis results, which account for the localizations and masses of the three transients, provide significantly robust support for the hypothesis of a common origin (\mathcal{H}_1). Moreover, we reanalyze the potential association by including the spins of the gravitational wave events. However, we find that the spins do not contribute significant information, yielding a Bayes factor of approximately 1.03 for the spin-only model.

IV. CONCLUSIONS AND DISCUSSION

In this work, we investigate the potential association between GW190514 and GW190521 as a hierarchical triple merger associated with ZTF19abannhr, taking into account of sky position, distance, and mass of the sources using a Bayesian criterion. Although the previous study has shown that GW190514 and GW190521 are a plausible hierarchical triple merger, their analysis is not significant with p -value of ~ 0.14 [3] (generally, p -value of ≤ 0.05 is considered ‘significant’). Here, we introduce a new approach and propose using multi-messenger [4] signals to analyze the probability of the GW190514-GW190521 hi-

TABLE I. Model comparison results. The model \mathcal{H}_0 : $\{a, b, c\}$ refers to the scenario where the three detections are unrelated. The model \mathcal{H}_1 : $\{a-b-c\}$ corresponds to the case where the three detections share a common origin. In contrast, the models \mathcal{H}_2 , \mathcal{H}_3 , and \mathcal{H}_4 : $\{a-b, c\}$ mean that two of the detections (i.e., a and b) share a common source. The values in parentheses correspond to hypothetical models with the primary mass information in the AGN formation channel. The log Bayes factors are relative to the model \mathcal{H}_0 .

Models	Prior-odds	Log-Bayes-factors	Odds
\mathcal{H}_0 : GW190514, GW190521, ZTF19abahr	-	0	-
\mathcal{H}_1 : GW190514-GW190521-ZTF19abahr	10^{-5}	16.8(21.5)	199(21772)
\mathcal{H}_2 : GW190514-GW190521, ZTF19abahr	1/1000	5.9	0.4
\mathcal{H}_3 : GW190514-ZTF19abahr, GW190521	1/13	3.6(4.1)	3(5)
\mathcal{H}_4 : GW190521-ZTF19abahr, GW190514	1/13	4.9(7.8)	11(180)

erarchical triple merger. Our analysis (considering the primary masses) results greatly increase the probability, finding that a log Bayes factor of $\log \mathcal{B} = 16.8$ (21.5), corresponding to an odds ratio of $\mathcal{O} \sim 199$ (2×10^4): 1, assuming an astrophysical prior odds of $\mathcal{P} \sim 10^{-5}$. This suggest strong evidence for the first hierarchical triple merger associated with an electromagnetic counterpart in the AGN formation channel. The finding of the multi-messenger hierarchical triple merger in the AGN is crucial for understanding the formation mechanisms of massive black holes, the role of AGNs in hierarchical mergers, and the implications of multi-messenger astronomy

We show that the GW190514-GW190521 pair, which is separated by only one week, further supports the scenario of a triple hierarchical merger chain if associated with ZTF19abahr: i) Such a short time frame between the two mergers presents significant challenges for the reformation of a binary system and its subsequent merger. However, AGNs provide an environment conducive to overcoming these challenges [48, 49]. Specifically, the number density of black holes in the migration traps [35] of AGN disks is notably high due to migration [50]. This high density facilitates the rapid reformation of a binary system from GW190514’s remnant black holes, enabling a swift second merger with the aid of the dense gas in AGN disks; ii) GW190521 may not have had sufficient time to circularize in such a short interval, suggesting that it is likely to be eccentric [51, 52]. This inference is supported by previous analyses indicating a non-zero eccentricity for GW190521 [3], and AGN disk environments are known to promote an excess of eccentric mergers [16]. Our current methodological framework explicitly excludes time delay and eccentricity considerations in the statistical analysis, as these require dedicated waveform development that will be addressed in subsequent studies. Furthermore, we anticipate environmental effects to induce luminosity distance corrections of $\lesssim 1\%$ — a systematic uncertainty. This is tiny compared to the uncertainty in intrinsic luminosity distance for each binary black hole observation (typically $\pm 30\%$). The im-

pact warrants future investigation through targeted parameter estimation studies.

V. ACKNOWLEDGMENTS

This work is supported by National Key R&D Program of China (2020YFC2201400), the National Natural Science Foundation of China (grant No. 11922303), and the Fundamental Research Funds for the Central Universities, Wuhan University (grant No. 2042022kf1182). We use the gravitational wave datasets released with GWTC-2.1 [2], labeled as “cosm” and “IMRPhenomXPHM.” This research has made use of data or software obtained from the Gravitational Wave Open Science Center (<https://gwosc.org>), a service of the LIGO Scientific Collaboration, the Virgo Collaboration, and KAGRA. This material is based upon work supported by NSF’s LIGO Laboratory which is a major facility fully funded by the National Science Foundation, as well as the Science and Technology Facilities Council (STFC) of the United Kingdom, the Max-Planck-Society (MPS), and the State of Niedersachsen/Germany for support of the construction of Advanced LIGO and construction and operation of the GEO600 detector. Additional support for Advanced LIGO was provided by the Australian Research Council. Virgo is funded, through the European Gravitational Observatory (EGO), by the French Centre National de Recherche Scientifique (CNRS), the Italian Istituto Nazionale di Fisica Nucleare (INFN) and the Dutch Nikhef, with contributions by institutions from Belgium, Germany, Greece, Hungary, Ireland, Japan, Monaco, Poland, Portugal, Spain. KAGRA is supported by Ministry of Education, Culture, Sports, Science and Technology (MEXT), Japan Society for the Promotion of Science (JSPS) in Japan; National Research Foundation (NRF) and Ministry of Science and ICT (MSIT) in Korea; Academia Sinica (AS) and National Science and Technology Council (NSTC) in Taiwan. This analysis was made possible following software packages: NumPy [53], SciPy [54], Matplotlib [55], emcee [56], IPython [57], corner [58], seaborn [59], and Astropy [60].

[1] R. Abbott, T. D. Abbott, S. Abraham, F. Acernese, K. Ackley, C. Adams, R. X. Adhikari, V. B. Adya, C. Af-

feldt, M. Agathos, and et al., *Phys. Rev. Lett.* **125**,

- 101102 (2020), [arXiv:2009.01075 \[gr-qc\]](#).
- [2] R. Abbott, T. D. Abbott, F. Acernese, K. Ackley, C. Adams, N. Adhikari, R. X. Adhikari, V. B. Adya, C. Affeldt, D. Agarwal, and et al., *Phys. Rev. D* **109**, 022001 (2024), [arXiv:2108.01045 \[gr-qc\]](#).
- [3] D. Veske, A. G. Sullivan, Z. Márka, I. Bartos, K. R. Corley, J. Samsing, R. Busicchio, and S. Márka, *Astrophys. J.* **907**, L48 (2021), [arXiv:2011.06591 \[astro-ph.HE\]](#).
- [4] M. J. Graham, K. E. S. Ford, B. McKernan, N. P. Ross, D. Stern, K. Burdge, M. Coughlin, S. G. Djorgovski, A. J. Drake, D. Duev, M. Kasliwal, A. A. Mahabal, S. van Velzen, J. Belecki, E. C. Bellm, R. Burruss, S. B. Cenko, V. Cunningham, G. Helou, S. R. Kulkarni, F. J. Masci, T. Prince, D. Reiley, H. Rodriguez, B. Rusholme, R. M. Smith, and M. T. Soumagnac, *Phys. Rev. Lett.* **124**, 251102 (2020), [arXiv:2006.14122 \[astro-ph.HE\]](#).
- [5] S. L. Morton, S. Rinaldi, A. Torres-Orjuela, A. Derdzinski, M. P. Vaccaro, and W. Del Pozzo, *Phys. Rev. D* **108**, 123039 (2023), [arXiv:2310.16025 \[gr-qc\]](#).
- [6] J. Calderón Bustillo, S. H. W. Leong, K. Chandra, B. McKernan, and K. E. S. Ford, *arXiv e-prints*, [arXiv:2112.12481 \(2021\)](#), [arXiv:2112.12481 \[gr-qc\]](#).
- [7] A. Palmese, M. Fishbach, C. J. Burke, J. Annis, and X. Liu, *Astrophys. J.* **914**, L34 (2021), [arXiv:2103.16069 \[astro-ph.HE\]](#).
- [8] G. Ashton, K. Ackley, I. M. Hernandez, and B. Piotrkowski, *Classical and Quantum Gravity* **38**, 235004 (2021), [arXiv:2009.12346 \[astro-ph.HE\]](#).
- [9] Y. Yang, I. Bartos, V. Gayathri, K. E. S. Ford, Z. Haiman, S. Klimentenko, B. Kocsis, S. Márka, Z. Márka, B. McKernan, and R. O’Shaughnessy, *Phys. Rev. Lett.* **123**, 181101 (2019), [arXiv:1906.09281 \[astro-ph.HE\]](#).
- [10] G.-P. Li, *Phys. Rev. D* **105**, 063006 (2022), [arXiv:2202.09961 \[astro-ph.HE\]](#).
- [11] G.-P. Li, D.-B. Lin, and Y. Yuan, *Phys. Rev. D* **107**, 063007 (2023), [arXiv:2211.11150 \[astro-ph.HE\]](#).
- [12] B. McKernan, K. E. S. Ford, I. Bartos, M. J. Graham, W. Lyra, S. Marka, Z. Marka, N. P. Ross, D. Stern, and Y. Yang, *Astrophys. J.* **884**, L50 (2019), [arXiv:1907.03746 \[astro-ph.HE\]](#).
- [13] J.-M. Wang, J.-R. Liu, L. C. Ho, Y.-R. Li, and P. Du, *Astrophys. J.* **916**, L17 (2021), [arXiv:2106.07334 \[astro-ph.HE\]](#).
- [14] H. Tagawa, S. S. Kimura, Z. Haiman, R. Perna, and I. Bartos, *Astrophys. J.* **950**, 13 (2023), [arXiv:2301.07111 \[astro-ph.HE\]](#).
- [15] K. Chen and Z.-G. Dai, *Astrophys. J.* **961**, 206 (2024), [arXiv:2311.10518 \[astro-ph.HE\]](#).
- [16] J. Samsing, I. Bartos, D. J. D’Orazio, Z. Haiman, B. Kocsis, N. W. C. Leigh, B. Liu, M. E. Pessah, and H. Tagawa, *Nature (London)* **603**, 237 (2022), [arXiv:2010.09765 \[astro-ph.HE\]](#).
- [17] LIGO Scientific Collaboration, J. Aasi, B. P. Abbott, R. Abbott, T. Abbott, M. R. Abernathy, K. Ackley, C. Adams, T. Adams, P. Addesso, and et al., *Classical and Quantum Gravity* **32**, 074001 (2015), [arXiv:1411.4547 \[gr-qc\]](#).
- [18] F. Acernese, M. Agathos, K. Agatsuma, D. Aisa, N. Allemandou, A. Allocca, J. Amarni, P. Astone, G. Balestri, G. Ballardin, and et al., *Classical and Quantum Gravity* **32**, 024001 (2015), [arXiv:1408.3978 \[gr-qc\]](#).
- [19] E. C. Bellm, S. R. Kulkarni, M. J. Graham, R. Dekany, R. M. Smith, R. Riddle, F. J. Masci, G. Helou, T. A. Prince, S. M. Adams, C. Barbarino, T. Barlow, J. Bauer, R. Beck, J. Belicki, R. Biswas, N. Blagorodnova, D. Bodewits, B. Bolin, V. Brinnel, T. Brooke, B. Bue, M. Bulla, R. Burruss, S. B. Cenko, C.-K. Chang, A. Connolly, M. Coughlin, J. Cromer, V. Cunningham, K. De, A. Delacroix, V. Desai, D. A. Duev, G. Eadie, T. L. Farnham, M. Feeney, U. Feindt, D. Flynn, A. Franckowiak, S. Frederick, C. Fremling, A. Gal-Yam, S. Gezari, M. Giomi, D. A. Goldstein, V. Z. Golkhou, A. Goobar, S. Groom, E. Hacıopians, D. Hale, J. Henning, A. Y. Q. Ho, D. Hover, J. Howell, T. Hung, D. Huppenkothen, D. Imel, W.-H. Ip, Željko Ivezić, E. Jackson, L. Jones, M. Juric, M. M. Kasliwal, S. Kaspi, S. Kaye, M. S. P. Kelley, M. Kowalski, E. Kramer, T. Kupfer, W. Landry, R. R. Laher, C.-D. Lee, H. W. Lin, Z.-Y. Lin, R. Lunnan, M. Giomi, A. Mahabal, P. Mao, A. A. Miller, S. Monkewitz, P. Murphy, C.-C. Ngeow, J. Nordin, P. Nugent, E. Ofek, M. T. Patterson, B. Penprase, M. Porter, L. Rauch, U. Rebbapragada, D. Reiley, M. Rigault, H. Rodriguez, J. van Roestel, B. Rusholme, J. van Santen, S. Schulze, D. L. Shupe, L. P. Singer, M. T. Soumagnac, R. Stein, J. Surace, J. Sollerman, P. Szkody, F. Taddia, S. Terek, A. V. Sistine, S. van Velzen, W. T. Vestrand, R. Walters, C. Ward, Q.-Z. Ye, P.-C. Yu, L. Yan, and J. Zolkower, *Publications of the Astronomical Society of the Pacific* **131**, 018002 (2018).
- [20] M. J. Graham, B. McKernan, K. E. S. Ford, D. Stern, S. G. Djorgovski, M. Coughlin, K. B. Burdge, E. C. Bellm, G. Helou, A. A. Mahabal, F. J. Masci, J. Purdum, P. Rosnet, and B. Rusholme, *Astrophys. J.* **942**, 99 (2023), [arXiv:2209.13004 \[astro-ph.HE\]](#).
- [21] Planck Collaboration, N. Aghanim, Y. Akrami, M. Ashdown, J. Aumont, C. Baccigalupi, M. Ballardini, A. J. Banday, R. B. Barreiro, N. Bartolo, S. Basak, R. Battye, K. Benabed, J. P. Bernard, M. Bersanelli, P. Bielewicz, J. J. Bock, J. R. Bond, J. Borrill, F. R. Bouchet, F. Boulanger, M. Bucher, C. Burigana, R. C. Butler, E. Calabrese, J. F. Cardoso, J. Carron, A. Challinor, H. C. Chiang, J. Chluba, L. P. L. Colombo, C. Combet, D. Contreras, B. P. Crill, F. Cuttaia, P. de Bernardis, G. de Zotti, J. Delabrouille, J. M. Delouis, E. Di Valentino, J. M. Diego, O. Doré, M. Douspis, A. Ducout, X. Dupac, S. Dusini, G. Efstathiou, F. Elsner, T. A. Enßlin, H. K. Eriksen, Y. Fantaye, M. Farhang, J. Ferguson, R. Fernandez-Cobos, F. Finelli, F. Forastieri, M. Frailis, A. A. Fraisse, E. Franceschi, A. Frolov, S. Galeotta, S. Galli, K. Ganga, R. T. Génova-Santos, M. Gerbino, T. Ghosh, J. González-Nuevo, K. M. Górski, S. Gratton, A. Gruppuso, J. E. Gudmundsson, J. Hamann, W. Handley, F. K. Hansen, D. Herranz, S. R. Hildebrandt, E. Hivon, Z. Huang, A. H. Jaffe, W. C. Jones, A. Karakci, E. Keihänen, R. Keskitalo, K. Kiiveri, J. Kim, T. S. Kisner, L. Knox, N. Krachmalnicoff, M. Kunz, H. Kurki-Suonio, G. Lagache, J. M. Lamarre, A. Lasenby, M. Lattanzi, C. R. Lawrence, M. Le Jeune, P. Lemos, J. Lesgourgues, F. Levrier, A. Lewis, M. Liguori, P. B. Lilje, M. Lilley, V. Lindholm, M. López-Cañiego, P. M. Lubin, Y. Z. Ma, J. F. Macías-Pérez, G. Maggio, D. Maino, N. Mandolesi, A. Mangilli, A. Marcos-Caballero, M. Maris, P. G. Martin, M. Martinelli, E. Martínez-González, S. Matarrese, N. Mauri, J. D. McEwen, P. R. Meinhold, A. Melchiorri, A. Mennella, M. Migliaccio, M. Millea, S. Mitra, M. A. Miville-Deschênes, D. Molinari, L. Montier, G. Morgante, A. Moss, P. Natoli, H. U.

- Nørgaard-Nielsen, L. Pagano, D. Paoletti, B. Partridge, G. Patanchon, H. V. Peiris, F. Perrotta, V. Pettorino, F. Piacentini, L. Polastri, G. Polenta, J. L. Puget, J. P. Rachen, M. Reinecke, M. Remazeilles, A. Renzi, G. Rocha, C. Rosset, G. Roudier, J. A. Rubiño-Martín, B. Ruiz-Granados, L. Salvati, M. Sandri, M. Savelainen, D. Scott, E. P. S. Shellard, C. Sirignano, G. Sirri, L. D. Spencer, R. Sunyaev, A. S. Suur-Uski, J. A. Tauber, D. Tavagnacco, M. Tenti, L. Toffolatti, M. Tomasi, T. Trombetti, L. Valenziano, J. Valiviita, B. Van Tent, L. Vibert, P. Vielva, F. Villa, N. Vittorio, B. D. Wandelt, I. K. Wehus, M. White, S. D. M. White, A. Zachei, and A. Zonca, *Astron. Astrophys* **641**, A6 (2020), arXiv:1807.06209 [astro-ph.CO].
- [22] A. R. King, J. E. Pringle, and J. A. Hofmann, *Mon. Not. R. Astron. Soc.* **385**, 1621 (2008), arXiv:0801.1564 [astro-ph].
- [23] B. Liu, D. Lai, and Y.-H. Wang, *Astrophys. J.* **883**, L7 (2019), arXiv:1906.07726 [astro-ph.HE].
- [24] Y. Fang and Q.-G. Huang, *Phys. Rev. D* **99**, 103005 (2019), arXiv:1901.05591 [gr-qc].
- [25] X. Chen and Z. Zhang, *Phys. Rev. D* **106**, 103040 (2022), arXiv:2206.08104 [astro-ph.HE].
- [26] G. Fabj, S. S. Nasim, F. Caban, K. E. S. Ford, B. McKernan, and J. M. Bellovary, *Mon. Not. R. Astron. Soc.* **499**, 2608 (2020), arXiv:2006.11229 [astro-ph.GA].
- [27] H. Yan, X. Chen, and A. Torres-Orjuela, *Phys. Rev. D* **107**, 103044 (2023), arXiv:2305.04969 [gr-qc].
- [28] L. Gualtieri, E. Berti, V. Cardoso, and U. Sperhake, *Phys. Rev. D* **78**, 044024 (2008), arXiv:0805.1017 [gr-qc].
- [29] M. Boyle, *Phys. Rev. D* **93**, 084031 (2016), arXiv:1509.00862 [gr-qc].
- [30] A. Torres-Orjuela, X. Chen, and P. Amaro Seoane, *Phys. Rev. D* **104**, 123025 (2021), arXiv:2010.15856 [astro-ph.CO].
- [31] X. Chen, S. Li, and Z. Cao, *Mon. Not. R. Astron. Soc.* **485**, L141 (2019), arXiv:1703.10543 [astro-ph.HE].
- [32] A. Torres-Orjuela and X. Chen, *Phys. Rev. D* **107**, 043027 (2023), arXiv:2210.09737 [astro-ph.CO].
- [33] B. Gao, S.-P. Tang, J. Yan, and Y.-Z. Fan, *Astrophys. J.* **965**, 80 (2024), arXiv:2402.17381 [gr-qc].
- [34] S.-P. Tang, Y.-Z. Fan, and D.-M. Wei, *Mon. Not. R. Astron. Soc.* **523**, 4113 (2023), arXiv:2209.03631 [gr-qc].
- [35] J. M. Bellovary, M.-M. Mac Low, B. McKernan, and K. E. S. Ford, *Astrophys. J.* **819**, L17 (2016), arXiv:1511.00005 [astro-ph.GA].
- [36] P. Peng and X. Chen, *Mon. Not. R. Astron. Soc.* **505**, 1324 (2021), arXiv:2104.07685 [astro-ph.HE].
- [37] Y. Wu, Y.-X. Chen, and D. N. C. Lin, *Mon. Not. R. Astron. Soc.* **528**, L127 (2024), arXiv:2311.15747 [astro-ph.EP].
- [38] E. Grishin, S. Gilbaum, and N. C. Stone, *Mon. Not. R. Astron. Soc.* **530**, 2114 (2024), arXiv:2307.07546 [astro-ph.HE].
- [39] R. Abbott, T. D. Abbott, F. Acernese, K. Ackley, C. Adams, N. Adhikari, R. X. Adhikari, V. B. Adya, C. Affeldt, D. Agarwal, and et al., *Physical Review X* **13**, 011048 (2023), arXiv:2111.03634 [astro-ph.HE].
- [40] Y. Yang, I. Bartos, Z. Haiman, B. Kocsis, Z. Márka, N. C. Stone, and S. Márka, *Astrophys. J.* **876**, 122 (2019), arXiv:1903.01405 [astro-ph.HE].
- [41] B. McKernan, K. E. S. Ford, R. O'Shaughnessy, and D. Wysocki, *Mon. Not. R. Astron. Soc.* **494**, 1203 (2020), arXiv:1907.04356 [astro-ph.HE].
- [42] E. Barausse, V. Morozova, and L. Rezzolla, *Astrophys. J.* **758**, 63 (2012), arXiv:1206.3803 [gr-qc].
- [43] F. Hofmann, E. Barausse, and L. Rezzolla, *Astrophys. J.* **825**, L19 (2016), arXiv:1605.01938 [gr-qc].
- [44] M. Campanelli, C. Lousto, Y. Zlochower, and D. Merritt, *Astrophys. J.* **659**, L5 (2007), arXiv:gr-qc/0701164 [gr-qc].
- [45] A. Heger, C. L. Fryer, S. E. Woosley, N. Langer, and D. H. Hartmann, *Astrophys. J.* **591**, 288 (2003), arXiv:astro-ph/0212469 [astro-ph].
- [46] S. E. Woosley, S. Blinnikov, and A. Heger, *Nature (London)* **450**, 390 (2007), arXiv:0710.3314 [astro-ph].
- [47] R. Abbott, T. D. Abbott, S. Abraham, F. Acernese, K. Ackley, C. Adams, R. X. Adhikari, V. B. Adya, C. Affeldt, M. Agathos, and et al., *Astrophys. J.* **900**, L13 (2020), arXiv:2009.01190 [astro-ph.HE].
- [48] I. Bartos, B. Kocsis, Z. Haiman, and S. Márka, *Astrophys. J.* **835**, 165 (2017), arXiv:1602.03831 [astro-ph.HE].
- [49] B. McKernan, K. E. S. Ford, J. Bellovary, N. W. C. Leigh, Z. Haiman, B. Kocsis, W. Lyra, M. M. Mac Low, B. Metzger, M. O'Dowd, S. Endlich, and D. J. Rosen, *Astrophys. J.* **866**, 66 (2018), arXiv:1702.07818 [astro-ph.HE].
- [50] B. McKernan, K. E. S. Ford, W. Lyra, and H. B. Perets, *Mon. Not. R. Astron. Soc.* **425**, 460 (2012), arXiv:1206.2309 [astro-ph.GA].
- [51] V. Gayathri, J. Healy, J. Lange, B. O'Brien, M. Szczepańczyk, I. Bartos, M. Campanelli, S. Klimentko, C. O. Lousto, and R. O'Shaughnessy, *Nature Astronomy* **6**, 344 (2022).
- [52] I. Romero-Shaw, P. D. Lasky, E. Thrane, and J. Calderón Bustillo, *Astrophys. J.* **903**, L5 (2020), arXiv:2009.04771 [astro-ph.HE].
- [53] C. R. Harris, K. J. Millman, S. J. van der Walt, R. Gommers, P. Virtanen, D. Cournapeau, E. Wieser, J. Taylor, S. Berg, N. J. Smith, R. Kern, M. Picus, S. Hoyer, M. H. van Kerkwijk, M. Brett, A. Haldane, J. F. del Río, M. Wiebe, P. Peterson, P. Gérard-Marchant, K. Sheppard, T. Reddy, W. Weckesser, H. Abbasi, C. Gohlke, and T. E. Oliphant, *Nature* **585**, 357 (2020).
- [54] P. Virtanen, R. Gommers, T. E. Oliphant, M. Haberland, T. Reddy, D. Cournapeau, E. Burovski, P. Peterson, W. Weckesser, J. Bright, S. J. van der Walt, M. Brett, J. Wilson, K. J. Millman, N. Mayorov, A. R. J. Nelson, E. Jones, R. Kern, E. Larson, C. J. Carey, Í. Polat, Y. Feng, E. W. Moore, J. VanderPlas, D. Laxalde, J. Perktold, R. Cimrman, I. Henriksen, E. A. Quintero, C. R. Harris, A. M. Archibald, A. H. Ribeiro, F. Pedregosa, P. van Mulbregt, and SciPy 1.0 Contributors, *Nature Methods* **17**, 261 (2020).
- [55] J. D. Hunter, *Computing in Science and Engineering* **9**, 90 (2007).
- [56] D. Foreman-Mackey, D. W. Hogg, D. Lang, and J. Goodman, *Publications of the Astronomical Society of the Pacific* **125**, 306 (2013), arXiv:1202.3665 [astro-ph.IM].
- [57] F. Perez and B. E. Granger, *Computing in Science and Engineering* **9**, 21 (2007).
- [58] D. Foreman-Mackey, *The Journal of Open Source Software* **1**, 24 (2016).
- [59] M. L. Waskom, *Journal of Open Source Software* **6**, 3021 (2021).
- [60] Astropy Collaboration, A. M. Price-Whelan, P. L. Lim, N. Earl, N. Starkman, L. Bradley, D. L. Shupe, A. A.

Patil, L. Corrales, C. E. Brasseur, M. Nöthe, A. Donath, E. Tollerud, B. M. Morris, A. Ginsburg, E. Vaher, B. A. Weaver, J. Tocknell, W. Jamieson, M. H. van Kerkwijk, T. P. Robitaille, B. Merry, M. Bachetti, H. M. Günther, T. L. Aldcroft, J. A. Alvarado-Montes, A. M. Archibald, A. Bódi, S. Bapat, G. Barentsen, J. Bazán, M. Biswas, M. Boquien, D. J. Burke, D. Cara, M. Cara, K. E. Conroy, S. Conseil, M. W. Craig, R. M. Cross, K. L. Cruz, F. D'Eugenio, N. Dencheva, H. A. R. Devillepoix, J. P. Dietrich, A. D. Eigenbrot, T. Erben, L. Ferreira, D. Foreman-Mackey, R. Fox, N. Freij, S. Garg, R. Geda, L. Glattly, Y. Gondhalekar, K. D. Gordon, D. Grant, P. Greenfield, A. M. Groener, S. Guest, S. Gurovich, R. Handberg, A. Hart, Z. Hatfield-Dodds, D. Homeier, G. Hosseinzadeh, T. Jenness, C. K. Jones, P. Joseph, J. B. Kalmbach, E. Karamehmetoglu, M. Kałuszyński, M. S. P. Kelley, N. Kern, W. E. Kerzendorf, E. W. Koch, S. Kulumani, A. Lee, C. Ly, Z. Ma, C. MacBride, J. M. Maljaars, D. Muna, N. A. Murphy, H. Norman, R. O'Steen, K. A. Oman, C. Pacifici, S. Pascual, J. Pascual-Granado, R. R. Patil, G. I. Perren, T. E. Pickering, T. Rastogi, B. R. Roulston, D. F. Ryan, E. S. Rykoff, J. Sabater, P. Sakurikar, J. Salgado, A. Sanghi, N. Saunders, V. Savchenko, L. Schwardt, M. Seifert-Eckert, A. Y. Shih, A. S. Jain, G. Shukla, J. Sick, C. Simpson, S. Singanamalla, L. P. Singer, J. Singhal, M. Sinha, B. M. Sipócz, L. R. Spitler, D. Stansby, O. Streicher, J. Šumak, J. D. Swinbank, D. S. Taranu, N. Tewary, G. R. Tremblay, M. de Val-Borro, S. J. Van Kooten, Z. Vasović, S. Verma, J. V. de Miranda Cardoso, P. K. G. Williams, T. J. Wilson, B. Winkel, W. M. Wood-Vasey, R. Xue, P. Yoachim, C. Zhang, A. Zonca, and Astropy Project Contributors, *Astrophys. J.* **935**, 167 (2022), [arXiv:2206.14220](https://arxiv.org/abs/2206.14220) [astro-ph.IM].